Lipid Bilayers Driven to a Wrong Lane in Molecular Dynamics Simulations by Subtle Changes in Long-Range Electrostatic Interactions

Michael Patra and Mikko Karttunen

Biophysics and Statistical Mechanics Group, Laboratory of Computational Engineering, Helsinki University of Technology, P.O. Box 9203, FIN-02015 HUT, Finland

Marja T. Hyvönen

Wihuri Research Institute, Kalliolinnantie 4, FIN-00140 Helsinki, Finland, and Laboratory of Physics and Helsinki Institute of Physics, Helsinki University of Technology, P.O. Box 1100, FIN-02015 HUT, Finland

Emma Falck and Ilpo Vattulainen*

Laboratory of Physics and Helsinki Institute of Physics, Helsinki University of Technology, P.O. Box 1100, FIN-02015 HUT, Finland

Received: November 26, 2003

We provide compelling evidence that different treatments of electrostatic interactions in molecular dynamics simulations may dramatically affect dynamic properties of lipid bilayers. To this end, we consider a fully hydrated pure dipalmitoylphosphatidylcholine bilayer through 50-ns molecular dynamics simulations and study various dynamic properties of individual lipids in a membrane, including the velocity autocorrelation function, the lateral and rotational diffusion coefficients, and the autocorrelation function for the area per molecule. We compare the results based on the Particle-Mesh Ewald (PME) and reaction field (RF) techniques with those obtained by an approach where the electrostatic interactions are truncated at $r_{cut} = 1.8$, 2.0, and 2.5 nm. We find that the overall performance of PME is very good; its results are consistent with the expected behavior. The RF method performs rather well, too, despite certain inherent problems and the fact that its results differ from those obtained by PME. Nevertheless, the largest differences are found for the truncation methods, for which all examined truncation methods lead to results distinctly different from those obtained by PME. The lateral diffusion coefficients obtained by PME and truncation at 1.8 nm, for example, differ by a factor of 10, while the PME results are consistent with experimental values. The observed deviations can be interpreted in terms of artificial ordering due to truncation and highlight the important role of electrostatic interactions in the dynamics of systems composed of lipids and other biologically relevant molecules such as proteins and DNA.

1. Introduction

Electrostatics play a crucial role in numerous soft-matter systems, including the properties of water, structure of proteins and DNA, and self-assembly and overcharging of DNA−lipid complexes.[1−7] Lipids in particular are an excellent example since they form stable structures such as bilayers, which serve as mattresses for proteins embedded in cell membranes.[8−12] Furthermore, lipids are involved in processes such as gene- and drug-transfer facilitated by liposomes that are essentially lipid bilayers.[13,14]

In the above examples, the properties of biological systems in question are strongly influenced by *long-range electrostatic interactions*. This is a crucial issue in computational modeling, as techniques such as classical molecular dynamics (MD) have become a common tool for studies of macromolecular systems at an atomic level.[15,16] Thus, proper treatment of electrostatic interactions is acknowledged as one of the most important issues in MD simulations, and there has been a substantial amount of work to develop reliable and efficient methods to this end.[17]

In this regard, there are techniques such as the Ewald summation (and its variants)[18] and the fast multipole method,[15,19] which are based on solving the Poisson equation for the electrostatic potential such that all charged particles and their periodic images are taken into account in a systematic fashion. In particular, the Particle-Mesh Ewald (PME) technique[15,20] has been applied increasingly often in MD studies of soft-matter systems. Another commonly used technique that approximately accounts for the long-range nature of electrostatic interactions is the reaction field (RF) method,[21] which is based on a RF correction beyond some cutoff distance.

Alternatively, one can neglect the long-range Coulombic tail and truncate the interactions at some suitable distance, a typical choice being 1.4−2.0 nm. This approach is appealing since it leads to considerable savings in the computational cost. Consequently, it is frequently used when computational requirements are substantial due to large system sizes or long time scales, which may be the case, e.g., in studies of lipid−protein systems,[22] self-assembly of lipids,[23] and membrane fusion.[24] Unfortunately, this speed-up does not come for free. It has been shown that the truncation of electrostatics is associated with certain *artifacts in structural properties of biological molecules*.

* Author to whom correspondence may be addressed. E-mail: Ilpo.Vattulainen@csc.fi.

10.1021/jp031281a CCC: $27.50
Published on Web 03/13/2004

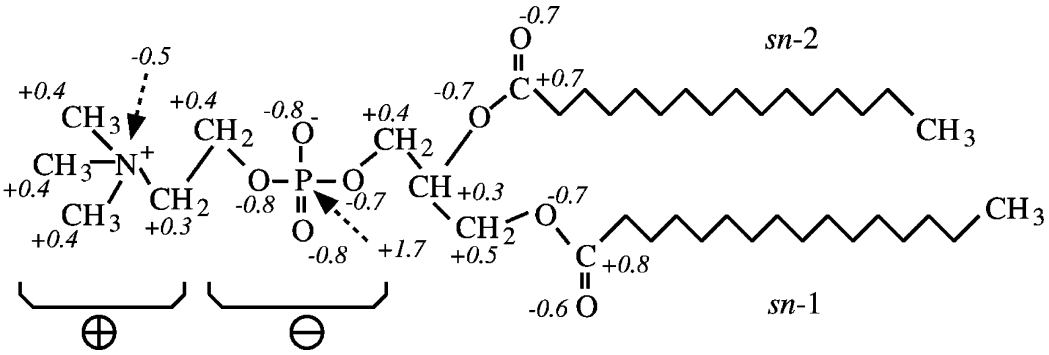

Figure 1. Representation of a DPPC molecule showing the magnitudes and locations of partial charges in the model.

For example, the structural properties of water both in bulk[25−27] and close to lipid monolayers[26,28,29] have been found to be affected by the truncation of electrostatic interactions. Other cases where similar structural effects have been observed include peptides,[30,31] proteins,[32] DNA,[33,34] and most recently lipid bilayers.[35,36]

In view of the importance of membranes for numerous cellular processes, it is very surprising that the influence of electrostatic interactions on *lipid bilayers* has been in the spotlight only very recently. Venable et al. considered a one-component dipalmitoylphosphatidylcholine (DPPC) bilayer in the low-temperature gel state using both PME and truncation at 1.2 nm, and found[35] that the results for the area per molecule differed by about 4%. Very recently, we focused on a DPPC bilayer in a physiologically more relevant liquid-crystalline phase and found that various structural properties exhibit major artifacts due to the truncation of electrostatic interactions.[36] For example, when the PME results were compared to those obtained using a truncation at 1.8 nm, the results for the area per lipid molecule differed by about 15%, and the results for the order parameter[37] characterizing the orientational order of lipid acyl chains (and related to the second Legendre polynomial) varied by about 45%. In both cases, the PME results were in agreement with experimental data. The size of these artifacts is simply astounding, yet the underlying reason is very simple: Truncation leads to artificial ordering in the plane of the membrane,[36] which implies that the phase behavior of the system is different from the desired one. If this is the case, then it is clear that essentially all structural properties of any lipid bilayer system deviate from their true behavior. This conclusion is supported by recent methodological studies by Anézo et al.[38]

These findings give rise to the interesting question of how important is the proper treatment of electrostatic interactions for *dynamic properties* in biologically relevant soft-matter systems. Rather surprisingly, this question has not been addressed in the case of lipid bilayer systems at all, yet the dynamics of lipid bilayers play the key role in processes such as lateral diffusion, membrane fusion, and permeation. Because of the central role of membranes in regulating various cellular processes through the function of proteins, the correct description of electrostatics for membrane dynamics is particularly important. Besides this, during the last year or so dynamic properties of lipid systems have become a very topical issue since MD simulations of the order of 50−100 ns are now possible.[23,24] These time scales allow, for the first time, studies of complex dynamic processes associated with membranes, such as fusion and self-assembly, among others.

In this article, we show through an extensive set of 50-ns MD simulations for a fully hydrated pure lipid bilayer of 128 DPPC molecules in the liquid-crystalline phase that *truncation of electrostatic interactions can have dramatic consequences on the dynamic properties of lipid bilayer systems*. We consider several truncation distances from 1.8 to 2.5 nm and compare the results to those obtained using the PME and RF techniques. We consider several dynamic properties of individual lipid molecules, including the lateral and rotational diffusion as well as the autocorrelation function of the area per lipid. We find that both the RF and truncation methods lead to distinctly different results as compared to a case where PME has been applied. Interestingly, the *deviations were observed on all time scales studied*. The lateral diffusion serves as an excellent example of this fact, since while the PME result is consistent with experimental values, the RF technique yields a lateral diffusion coefficient three times larger than the PME result. For the truncation method, the situation is even more serious as the lateral diffusion coefficient for a truncation at 1.8 nm differed from the PME result by a factor of 10.

We conclude that the deviations between truncation and PME persist even for large truncation distances. This strongly suggests that the artifacts due to truncation are systematic and cannot be cured by increasing the cutoff distance. The performance of the RF technique, however, is considerably better. Yet, if the computational load is not a limiting factor, PME is the method of choice.

2. System

2.1. Model and Simulation Details. We have considered a one-component lipid bilayer consisting of $N = 128$ DPPC molecules fully hydrated by 3655 water molecules. The initial bilayer configuration made up of DPPC molecules corresponds to the final structure of run E presented in ref 39 (available at http://moose.bio.ucalgary.ca/files/dppc128.pdb), and the principal axes of the system are chosen such that the bilayer is in the *xy* plane. The united atom model description used in this work has been considered previously by Tieleman et al.[39] and validated in a more recent MD study.[36]

The parameters for bonded and nonbonded interactions were taken from a rather recent study on a DPPC bilayer system,[40] available in electronic form at http://moose.bio.ucalgary.ca/files/lipid.itp. The partial charges were obtained from the underlying model description[39] and can be found at http://moose.bio.ucalgary.ca/files/dppc.itp. For clarity's sake, they are also shown in Figure 1. For water, we used the SPC (single-point charge) model.[41]

An approach commonly adapted in lipid bilayer simulations is to calculate electrostatic interactions within a certain distance (usually about 1.0 nm) at each time step, while interactions beyond this range are determined every k time steps ($k \gg 1$). There are two commonly used approaches known as the multiple time step (MTS) and the twin-range cutoff (TRC) schemes. (The notations are not fully established and are discussed in ref 42.)

Both schemes evaluate long-range forces only once every k steps. In MTS, the velocities are updated in steps 1, ..., $k-1$ only from the short-range forces, and only during the step k is the velocity updated also from the long-range forces. In TRC the velocity is updated at each time step also from the long-range forces, though it is assumed to be constant within each cycle of k steps.

It can be expected that TRC should give slightly "more accurate" trajectories, while MTS offers the advantage that time-reversal symmetry is observed more appropriately than in the TRC scheme. For this reason, k is usually limited to about 10 in TRC, while MTS would allow significantly larger k.

In this work, we have used a scheme where electrostatic interactions within 1.0 nm were calculated at each time step, while interactions beyond this range were determined every $k = 10$ time steps by TRC. This choice is supported by a number of reasons. First, due to the relatively small k applied by us, the problem of how to best divide the forces into long-range and short-range components is not as important as in the MTS schemes. Second, these choices follow the parametrization of DPPC by Tieleman and Berendsen.[39] In addition, since basically all DPPC simulations reported so far have used a twin-range scheme and our objective is to use an approach that is common in this field, we decided to follow the same idea.

We have employed three different methods to take care of the long-range electrostatics. Group-based long-range electrostatic interactions were handled either by using a cutoff at $r_{cut} = 1.8$, 2.0, or 2.5 nm or by means of the PME[15,20] method to take the long-range interaction fully into account. In addition to these approaches, we considered the RF method[21] in which the electrostatic interaction is explicitly accounted for up to $r_{RF} = 0.9$ nm, beyond which the remaining long-range contribution is described by a (mean-field type) RF correction using a dielectric constant of $\epsilon_{RF} = 80$. This set of parameters is a common choice in MD simulations of lipid bilayers using the RF method for electrostatics.[43−45] Finally, Lennard-Jones interactions were cut off at 1.0 nm without switch functions.

The simulations were performed using the Gromacs[46] package in the *NpT* ensemble using a time step of 2.0 fs. The Berendsen algorithm with a time constant of 1 ps for pressure coupling was used as barostat. The setup was chosen such that the height of the simulation box (i.e., its extension in the z direction) was allowed to vary independently of the cross-sectional area of the box in the xy plane. The DPPC and water molecules were separately coupled to a heat bath at temperature $T = 323$ K using the Berendsen algorithm[47] with a coupling constant of 0.1 ps. The lengths of all bonds were kept constant with the Lincs algorithm.[48]

Typical time scales studied in recent MD simulations of lipid bilayer systems have been of the order of 3−20 ns.[43−45,49−52] These time scales can provide one with a great deal of insight into the structural properties of membrane systems. In the case of dynamics, however, the computational requirements are appreciably more demanding. In the present work, the simulations in each case have been extended over a time scale of 50 ns. While this time scale is large compared to the current trend, it is still relatively short compared to time scales associated with complex dynamic processes such as self-assembly and long-range undulations of lipid bilayers, which take place over time scales of the order of 100 ns.[23,53,54] Despite this shortcoming, we show below that the present multi-nanosecond study allows us to analyze various dynamic processes in full detail and to quantify artifacts in dynamic quantities due to the truncation of electrostatic interactions.

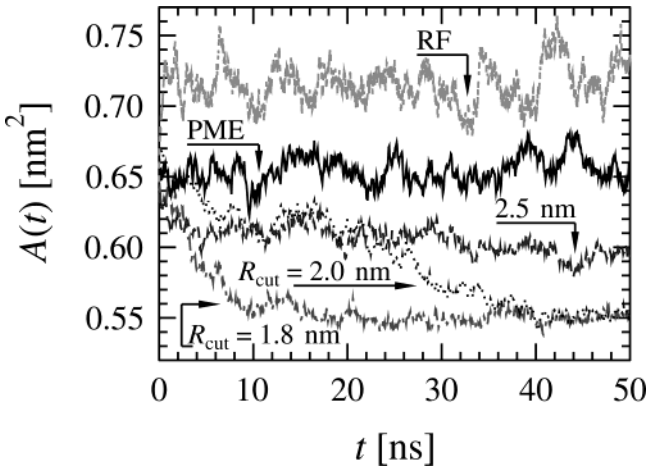

Figure 2. Evolution of the area per molecule in time.

The simulations reported in this work took about 25 000 CPU hours in total, using 2.4-GHz Pentium 4 processors. This includes simulations at different temperatures, with various coupling constants for the barostat and the thermostat, and with different truncation distances for van der Waals interactions to confirm the validity of our results.[36]

3. Results

To investigate the influence of how electrostatic interactions are accounted for on the dynamical properties of lipid membranes, we consider various dynamical quantities related to membranes. We focus on area fluctuations and the lateral and rotational diffusion of lipid molecules. Further diffusion processes such as permeation and flip-flops take place over much larger time scales and are therefore not considered in this work.

Note that the interactions used in the present work are entirely similar in all systems we have studied, except for the scheme chosen for the long-range electrostatic interactions. Thus, all differences discussed below are due to electrostatics. To facilitate the comparison, we have chosen to use the PME method as a reference to which the other approaches are compared. This choice is supported by the fact that its only known problem is related to the periodicity of the system, and this problem is expected to be smaller than the problems of other approaches considered in the present study.

3.1. Area per Molecule and Radial Distribution Functions. Before a thorough discussion of dynamics, let us first consider two important quantities that will shed some light on the origin of the artifacts. The first of them, the area per molecule, is a central quantity in membrane systems. Besides the fact that it is one of the few quantities that can be determined accurately from experiments, area fluctuations in a bilayer are related to the compressibility of the bilayer, which plays an important role in processes such as lateral diffusion, hole formation, and permeation. The second quantity, radial distribution function, in turn, is an important quantity in all soft-matter systems. By assumption that the structure of lipid bilayers is influenced by the way the electrostatics is treated in MD simulations, it is clear that the radial distribution function should show corresponding artifacts.

Results in Figure 2 illustrate the time dependence of the area per DPPC molecule $A(t)$ over a time scale of 50 ns. We find that the equilibration of $A(t)$ takes about 10 ns, and thus we have discarded this part of the trajectory and used only the last 40 ns for analysis. The simulations using PME yield $\langle A \rangle = (0.655 \pm 0.010)$ nm^2. This is consistent with recent experi-

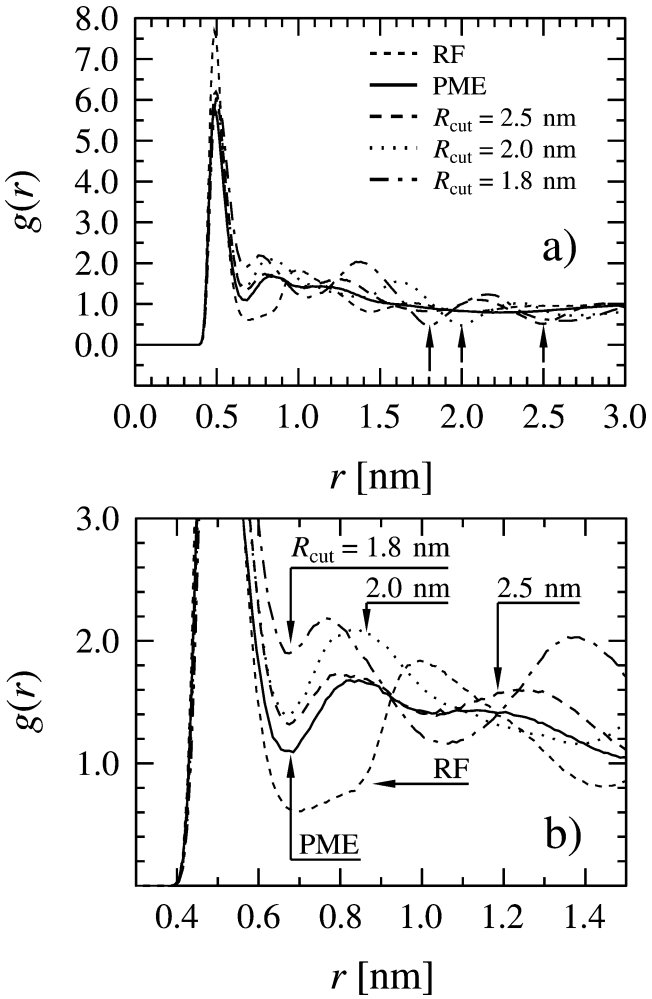

Figure 3. (a) Radial distribution function for intermolecular P−N pairs in the headgroups of the DPPC molecules. Note the dips exactly at the truncation distance as shown by the arrows. (b) Same as Figure 3a but now on an expanded scale to better illustrate the differences between different schemes.

ments,[11] which for DPPC give $\langle A \rangle = 0.64$ nm^2. The RF method yields $\langle A \rangle = (0.716 \pm 0.014)$ nm^2 that is about 9% larger than the PME result. Truncation at 2.5 nm leads to $\langle A \rangle = (0.604 \pm 0.009)$ nm^2, which deviates about 8% from the PME result. Decreasing the cutoff distance to 2.0 nm leads to $\langle A \rangle = (0.582 \pm 0.027)$ nm^2, which should be taken with some caution as the area per molecule in this case seems to have a systematic drift to smaller values. However, we found that $A(t)$ increases at times beyond 40 ns, indicating that the decrease of $A(t)$ between 20 and 40 ns is likely due to statistical fluctuations (see discussion in section 3.2). Finally, simulations using truncation at $r_{cut} = 1.8$ nm yielded $\langle A \rangle = (0.551 \pm 0.005)$ nm^2. We note that a recent study by Anézo et al.[38] focusing on the influence of electrostatics on the area per molecule is consistent with our findings.

The artifacts in the area per molecule, and in other structural quantities, are discussed in more detail in ref 36. Instead of discussing them any further in this work, we rather note that the artifacts when using the truncation methods are essentially due to truncation of electrostatics, which leads to artificial ordering in the plane of the membrane. This is demonstrated in Figure 3 by the intermolecular radial distribution function (RDF) $g(r)$ for the N−P pair between nitrogen and phosphate atoms in the headgroups. While PME yields an RDF which has essentially no structure beyond $r = 1.0$ nm, the RDFs of truncation schemes have a pronounced dip *exactly at the truncation distance*. As was shown in ref 36, similar conclusions on artificial ordering can be drawn for N−N and P−P pairs, in which cases the artifacts in the RDFs are even stronger. What is even more alarming is the fact that similar artificial peaks at r_{cut} were observed for the RDF of the center of mass (CM) positions of the lipids.[36]

As for the RF method, Figure 3 illustrates that its RDF is significantly different from that of PME. While both schemes yield the first minimum at about 0.68 nm, the pair correlation behavior of these two approaches is clearly different beyond this distance. In the present model system, the RDF based on the RF method has a weak oscillating long-range tail that extends up to about 2.5 nm, and a similar conclusion can be drawn on the basis of RDFs for N−N and P−P pairs (data available in Supporting Information). Then, it is not surprising that the RDF of the CM positions of the lipids was also found to be slightly but systematically different from its PME counterpart (data available in Supporting Information). Fortunately, the RDF of the RF method (for CM positions) does not indicate unphysical peaks. Rather, it decays rather rapidly as expected for a system in the liquid-crystalline (fluid) phase.

We conclude that the artifacts in structural quantities are due to the fact that the truncation method does not account for the long-range component of electrostatic interactions. Apparently, the truncation of electrostatic interactions gives rise to artificial ordering in the bilayer plane, thus changing the phase behavior of the system. The RF method performs considerably better in this respect, though its results are not fully consistent with those of PME. In the remaining part of this work, we investigate the influence of electrostatics on the *dynamics of a lipid bilayer*. As we will find, subtle differences in the electrostatic schemes lead to major differences in various dynamic quantities.

3.2. Decay of the Area Autocorrelation Function. As the first dynamic quantity, we consider the area fluctuations by following the autocorrelation function

$$C_A(t) \equiv \frac{1}{N}\sum_{i=1}^{N} \frac{\langle A_i(t+t')A_i(t')\rangle - \langle A_i\rangle^2}{\langle A_i^2\rangle - \langle A_i\rangle^2}, \qquad (1)$$

where $A_i(t)$ is the area of the molecule i ($i = 1, ..., N$) at time t, and $\langle\ \rangle$ denotes a time average over a large number of configurations. Notably, $C_A(t)$ describes fluctuations in the area of a single lipid molecule in the plane of the membrane. Assuming an asymptotic decay $C_A(t) \sim \exp(-t/\tau)$, the characteristic decay time τ is then indicative of the lifetime of excess free area between lipid molecules thereby providing a first-order estimate of the lifetime of small pores between neighboring lipid molecules, which in turn is related to permeation of solutes across membranes.

To calculate the area occupied by each individual lipid, $A_i(t)$, we applied the Voronoi analysis in two dimensions.[55] We first computed the CM positions for the lipids and projected them onto the *xy* plane separately for each leaflet of the bilayer. A point in the plane is then considered to belong to a particular Voronoi cell if it is closer to the projected CM of the lipid molecule associated with that cell than to any other CM position.

Results in Figure 4 show that the area autocorrelation function decays on a time scale of a few nanoseconds. After a narrow initial regime of about 0.5−1 ns, the decay of $C_A(t)$ follows an exponential via $C_A(t) \sim \exp(-t/\tau)$. For the characteristic decay time (τ), results shown in Table 1 indicate that the area autocorrelation function based on the RF method decays fastest,

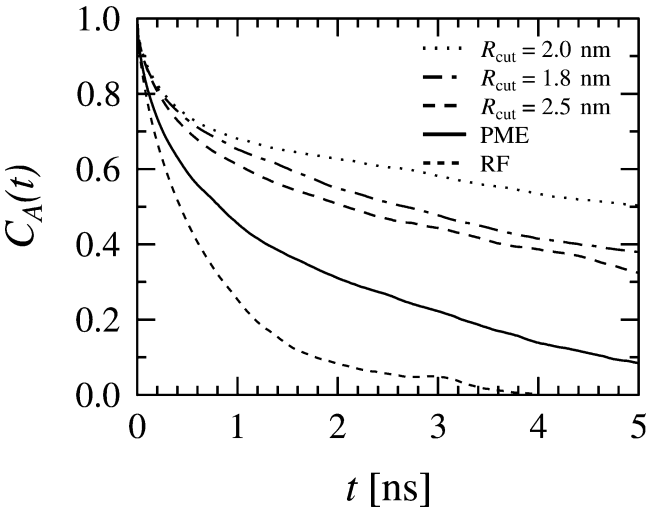

Figure 4. Results for the decay of the area autocorrelation function based on the Voronoi analysis in 2D.

TABLE 1: Characteristic Times τ and $t_{1/2}$ (in Units of Nanoseconds) Describing the Decay of the Area Autocorrelation Function $C_A(t)$

time	1.8 nm	2.0 nm	2.5 nm	PME	RF
τ	7.1 ± 0.6	12.3 ± 2.4	7.4 ± 2.7	2.5 ± 1.8	0.9 ± 0.2
$t_{1/2}$	2.7 ± 0.6	5.0 ± 0.6	2.1 ± 1.1	0.70 ± 0.07	0.43 ± 0.03

followed by PME, while the truncation schemes lead to a much slower decay. In addition, while the results of 1.8 and 2.5 nm are essentially identical, the case of 2.0 nm differs somewhat from the general trend. We expect that this is due to the drift of $A(t)$ in Figure 2, illustrating the common view that simulations using truncation are less stable compared to those using PME and its variants. This, too, should give rise to concern as it casts doubt for the commonly made estimates ($\sim$1−5 ns) of equilibration times in MD simulations of lipid bilayers. The autocorrelation times for area fluctuations shown in Table 1 support this idea. A further investigation of this issue would be highly interesting but is limited by the large time scales needed for this purpose, and is thus beyond the scope of this article.

As for the characteristic decay times, we find that the results of RF are significantly smaller than those of PME. For the truncation schemes, depending on the truncation distance, the characteristic decay time differs by a factor of 3−5 from the PME result. The half-times $t_{1/2}$ defined through $C_A(t_{1/2}) = {}^1/_2$ show the same trend (see Table 1). For comparison, we note that the PME result for $t_{1/2}$ is in agreement with the results of Shinoda and Okazaki,[55] who used Ewald summation for a DPPC bilayer.

The present results for the decay of area fluctuations allow us to conclude that the choice of electrostatics does influence the collective dynamics of lipid bilayers. In particular, as the correlation time of area fluctuations is significantly influenced by truncation, it is clear that it has implications for processes such as permeation through lipid bilayers.

3.3. Lateral Diffusion of Lipid Molecules. Lateral diffusion plays an important role in various physiologically important processes such as ordering of multicomponent lipid bilayers, endocytosis, and signaling within a lipid bilayer.[56,57] It is also one of the mechanisms that controls diffusion through membranes; e.g., the formation of ion channels is governed in part by the lateral diffusion of proteins embedded in a bilayer. As these examples illustrate, it is clear that lateral diffusion is one of the key processes that characterizes the dynamics of individual molecules in a cell membrane.

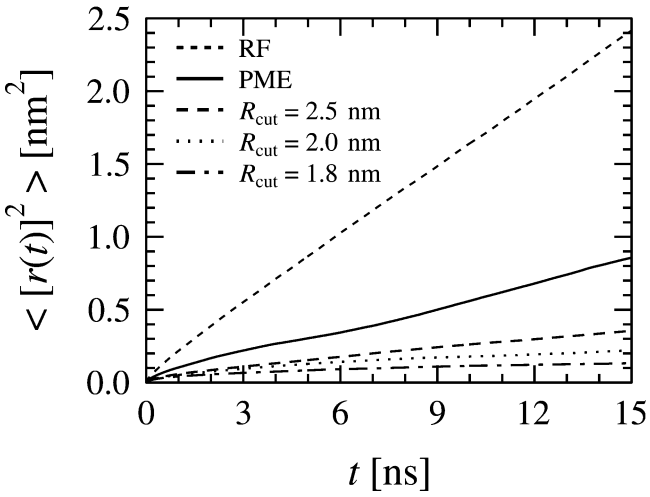

Figure 5. Results for the mean-square displacement in time.

To quantify the motion of single molecules in the plane of a membrane, let the CM position of lipid i at time t be $\vec{r}_i(t)$. The lateral diffusion coefficient is then defined through the Einstein relation[58]

$$D_T = \lim_{t\to\infty} \frac{1}{2dt} \langle [\vec{r}(t)]^2 \rangle \tag{2}$$

where $d = 2$ is the dimensionality of the bilayer and $\langle [\vec{r}(t)]^2 \rangle$ is the mean-squared displacement

$$\langle [\vec{r}(t)]^2 \rangle \equiv \frac{1}{N} \sum_{i=1}^{N} \langle [\vec{r}_i(t) - \vec{r}_i(0)]^2 \rangle \tag{3}$$

averaged over all the N molecules in a bilayer.

It is worthwhile pointing out that the center of mass positions of the two monolayers may fluctuate in time. If this drift is not accounted for, the results may reflect the motion of the monolayer's CM rather than the diffusion of individual molecules. We have paid particular attention to account for this matter by calculating the lateral diffusion coefficient in the absence of any flow; i.e., we follow the position of lipid i in the upper (lower) monolayer with respect to the CM position of the corresponding upper (lower) monolayer.

Results shown in Figure 5 for the mean-square displacement show that there are major differences between the different treatments of long-range electrostatic interactions. Deviations between the different cases appear already at short times and become increasingly apparent at longer times. When the long-time behavior is analyzed in detail in order to determine the lateral diffusion coefficient, we obtain the results shown in Table 2. It is evident that the lateral diffusion coefficient computed using RF is significantly larger than the lateral diffusion in the other cases. Further, the lateral diffusion from PME is substantially faster compared to cases based on the truncation of electrostatics. In particular, PME yields a lateral diffusion coefficient that is about *ten times larger* than the result found by truncation at 1.8 nm. For larger cutoff distances, we find that the lateral diffusion coefficients increase, though a systematic difference between truncation and PME results persists. Even for the largest truncation distance of 2.5 nm, which is about 40% of the linear system size in this case, the diffusion results deviate from PME by a factor of about 2.6.

For the present system, a systematic deviation between the PME and truncation results thus persists. If the system size were considerably larger, it might be that the truncation method with

TABLE 2: Lateral Diffusion Coefficients D_T Describing the Motion of DPPC Molecules in the Plane of the Bilayer[a]

electrostatics	D_T [cm^2/s]
truncation at 1.8 nm	$(1.3 \pm 0.3) \times 10^{-8}$
truncation at 2.0 nm	$(3.0 \pm 0.3) \times 10^{-8}$
truncation at 2.5 nm	$(4.9 \pm 0.4) \times 10^{-8}$
PME	$(12.7 \pm 0.5) \times 10^{-8}$
RF	$(41.1 \pm 1.6) \times 10^{-8}$
FRAP[65]	12.5×10^{-8}
QENS[66,67]	10×10^{-8}
FRAP[63]	13×10^{-8}

[a] Experimental values are also given for the purpose of comparison: FRAP experiments[65] for a DPPC bilayer at $T = 323$ K, QENS measurements[66,67] for a DPPC system at $T = 333$ K, and FRAP experiments[63] at $T = 323$ K for a DMPC system.

a large cutoff distance would yield results comparable to the PME results. However, this approach is not reasonable (see Section 3.7), besides which it is not clear that this idea would work at all. After all, the truncation neglects the long-range contribution beyond the cutoff region (taken into account by the Fourier-space part in PME).

The rate of lateral diffusion clearly depends on the average area per lipid $\langle A \rangle$. We find that the larger $\langle A \rangle$, the larger the lateral diffusion coefficient. This is in accord with the free-volume theory for lateral diffusion[59,60] and with experiments for single-component lipid bilayers.[61] (For results on $\langle A \rangle$ for the purpose of comparison, see, e.g., refs 11 and 62 and the discussions therein.) The differences in the lateral diffusion coefficients can therefore to a certain extent be traced back to the changes in structural aspects of the bilayer due to electrostatics.

The importance of the differences between PME and the other schemes can be illustrated by a brief comparison to experimental findings. Almeida et al. used the fluorescence recovery after photobleaching (FRAP) technique to measure lateral diffusion in a pure DMPC bilayer above the main transition temperature. They found that the lateral diffusion coefficient increased by a factor of 3.5 *if the temperature was increased by 32 °C* from 299 to 331 K.[63] For a DLPC−cholesterol bilayer mixture, Korlach et al. found[64] the lateral diffusion rate to decrease by a factor of 10 *if the cholesterol concentration was increased from 0 to 60%*. In these systems, the changes in lateral diffusion were caused by major changes in their thermodynamic state. In the present case, we have found changes of similar magnitude due to seemingly minor changes in electrostatic interactions. Thus, it is obvious that one should exercise great care when dealing with electrostatic interactions.

We would like to stress that different experimental techniques usually probe diffusion over a wide range of different time scales. As far as long-range diffusion over long time scales is concerned, the most appropriate comparison in the present case can be made to FRAP and "long-range" quasielastic neutron-scattering (QENS) measurements. Our findings using the PME scheme are consistent with these experimental values (see Table 2).

The present results demonstrate very clearly the subtle nature of electrostatic interactions. We have found that even seemingly minor changes in the treatment of electrostatic interactions can have dramatic consequences in transport coefficients defined over long times and large distances. The results based on RF and truncation are distinctly different from those obtained by PME. In particular, it is remarkable that even large cutoff distances comparable to the half of the linear size of the system lead to results systematically different from PME results.

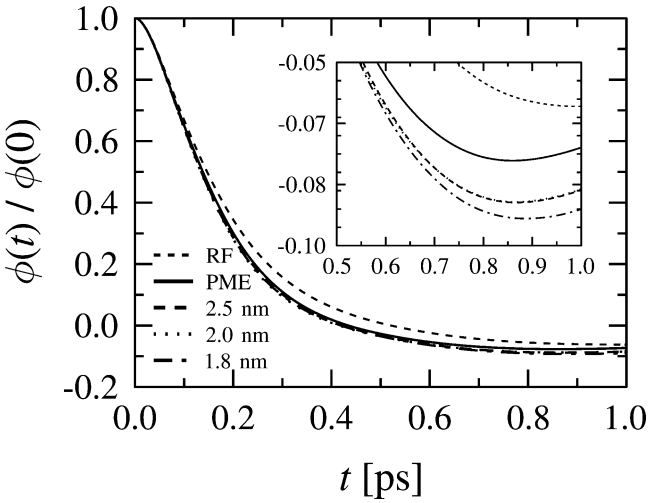

Figure 6. The normalized velocity autocorrelation function $\phi(t)/\phi(0)$ vs time. The deviations between the different schemes are illustrated in more detail in the inset. Note that the curve of 2.0 nm in the inset is essentially on top of the curve of 2.5 nm.

3.4. Velocity Autocorrelation Function. Alternatively, lateral diffusion of individual molecules can be described by the velocity autocorrelation function

$$\phi(t) \equiv \frac{1}{N} \sum_{i=1}^{N} \langle \vec{v}_i(t + t') \vec{v}_i(t') \rangle \tag{4}$$

where $\vec{v}_i(t)$ is the CM velocity of molecule i at time t. In principle, the lateral diffusion coefficient can then be defined through the Green−Kubo equation[58]

$$D_T = \frac{1}{d} \int_0^\infty \mathrm{d}t\, \phi(t) \tag{5}$$

In practice, however, this approach to calculate D_T is rather difficult due to the fact that the characteristic decay time of $\phi(t)$ is usually very small, whereas the convergence of the integral in eq 5 takes a long time. In the present case for a DPPC bilayer, we found that the characteristic decay time of $\phi(t)$ is about 0.2 ps, while the convergence was achieved on a time scale of the order of 2−5 ns. This implies that an accurate determination of D_T through eq 5 requires $\phi(t)$ to be sampled at very short time intervals up to large times, which is not meaningful.

We have used the velocity autocorrelation function to quantify the size of artifacts in dynamic quantities at *short times*. The diffusion behavior in this regime corresponds to motion known as "rattling in a cage", where the molecule in question goes through conformational changes, while its CM position does not fluctuate much compared to the size of the molecule in the bilayer plane. The short-time behavior thus complements the above results for the lateral diffusion coefficient describing dynamics over long times.

In Figure 6 we show the velocity autocorrelation function at short times up to 1 ps. In agreement with the results in section 3.3, the RF method yields the fastest diffusion rate. The difference between PME and the different truncation schemes is minor but systematic. The decay of $\phi(t)$ is fastest in the case of $r_{cut} = 1.8$ nm, followed by truncation distances of 2.0 and 2.5 nm, while PME leads to the slowest decay. As D_T is an integral of $\phi(t)$, these results are consistent with our findings in section 3.3.

TABLE 3: Effective Lateral Diffusion Coefficients D_{eff} Found by Integrating the Velocity Autocorrelation Function from (a) 0 to 1 ps and from (b) 0 to 10 ps (See Eq 5 and Figure 6)

electrostatics	D_{eff} (cm^2/s)
Case A	
truncation at 1.8 nm	$(6.13 \pm 0.11) \times 10^{-6}$
truncation at 2.0 nm	$(6.14 \pm 0.19) \times 10^{-6}$
truncation at 2.5 nm	$(6.26 \pm 0.08) \times 10^{-6}$
PME	$(6.76 \pm 0.06) \times 10^{-6}$
RF	$(8.39 \pm 0.11) \times 10^{-6}$
Case B	
truncation at 1.8 nm	$(1.11 \pm 0.04) \times 10^{-6}$
truncation at 2.0 nm	$(1.19 \pm 0.04) \times 10^{-6}$
truncation at 2.5 nm	$(1.23 \pm 0.03) \times 10^{-6}$
PME	$(1.57 \pm 0.02) \times 10^{-6}$
RF	$(2.12 \pm 0.03) \times 10^{-6}$

If we integrate $\phi(t)$ up to 1 ps (instead of very large times), we find effective diffusion coefficients D_{eff} on the scale of 6×10^{-6} cm^2/s (see Table 3). The RF method yields the largest value, which is about 24% larger than the PME result. The truncation methods lead to considerably slower diffusion, and the deviations between the truncation schemes compared to PME are also surprisingly large (7−10%) given that the time scale is very short and does not allow large displacements in the plane of the membrane. Nevertheless, the results imply that diffusion at very short time scales is not strongly influenced by the truncation of electrostatic interactions since the deviations in Table 3 are significantly smaller compared to those for lateral diffusion reported in Table 2 for D_T.

If $\phi(t)$ is considered up to 10 ps, one finds (see Table 3) the effective diffusion coefficients to be on a scale of 1×10^{-6} cm^2/s. The RF method yields an effective diffusion coefficient that is about 35% larger than the PME result, while the deviations between PME and the truncation schemes are about 21−29%. In this case, a direct comparison to experimental data is difficult, though the value 4×10^{-6} cm^2/s obtained by short-time ("local") QENS measurements[68] for DPPC at 336 K indicates that our results are on the same scale.

It is clear that the differences in the lateral diffusion coefficient D_T come mainly from the long-time behavior of $\phi(t)$, as the diffusion of lipid molecules becomes increasingly influenced by the artifacts due to electrostatics. The question is, do the deviations between the different schemes increase uniformly in time, or is there some characteristic time scale related to molecular diffusion mechanisms above which the artifacts in $\phi(t)$ become very pronounced over a short time scale? To address this question, we consider diffusion at different time scales in terms of lateral displacement distributions in section 3.5.

3.5. Distribution of Lateral Displacements. To clarify this issue, let us consider the distribution of particle displacement lengths over some fixed time scale. We denote the CM position of particle i at time t by $\vec{r}_i(t)$ and let it diffuse over a time period δt to position $\vec{r}_i(t + \delta t)$. Since the bilayer is in the xy plane, the projection of the particle position onto the bilayer plane, $\vec{r}_{i,2D}(t)$, defines the particle displacement $\delta\vec{r}_{i,2D}(\delta t) = \vec{r}_{i,2D}(t + \delta t) - \vec{r}_{i,2D}(t)$ whose length is denoted by $l_i(\delta t)$. As in section 3.3, the drift of the monolayer's CM has been accounted for in the analysis. The displacements $l_i(\delta t)$ make up a particle displacement distribution function $P_i(l,\delta t)$. When averaged over all the N molecules, one obtains $P(l,\delta t) = (1/N)\sum_{i=1}^{N} P_i(l, \delta t)$.

The second moment of $P(l,\delta t)$ at long times yields the lateral diffusion coefficient D_T. Here we use $P(l,\delta t)$ to quantify deviations between different cases by the average particle displacement

$$l_{ave}(\delta t) \equiv \int_0^\infty dl P(l,\delta t) l \qquad (6)$$

which describes how far, on average, a given particle moves during time δt. This is a suitable measure especially at short times: While quantities such as $(2dD_T\delta t)^{1/2}$ are often used for this purpose, they are valid only at large times in the diffusive regime, i.e., where $\langle[\vec{r}(t)]^2\rangle \sim t$.

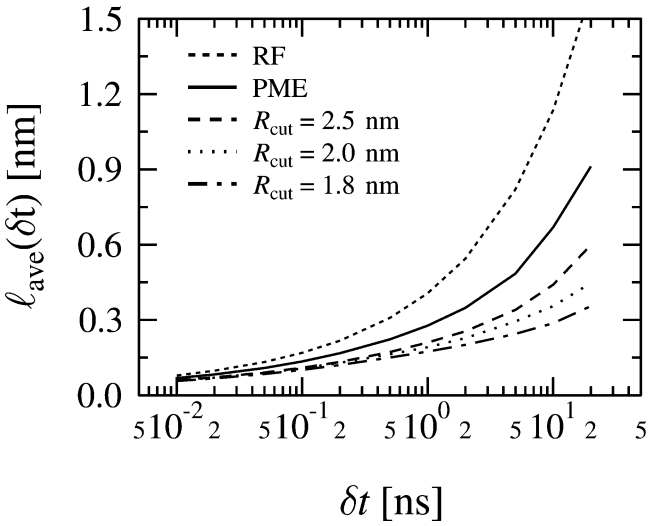

Figure 7. Average particle displacements $l_{ave}(\delta t)$ over a fixed time period δt.

The results for the average displacement $l_{ave}(\delta t)$ are summarized in Figure 7. It is clear that particle displacements are largest in the RF technique. As for the truncation schemes, for times up to $\delta t = 50$ ps, the average displacement obtained by the truncation schemes deviates by 15−30% from the PME result. At the same time, the results based on different truncation distances are approximately similar up to $\delta t = 100$ ps. Most remarkably, however, we find that the deviations between the different schemes increase uniformly in time.

Further studies of $P(l,\delta t)$ (data available in Supporting Information) indicate that it is strongly affected by the treatment of electrostatics. Already at short times of the order of 10 ps, the distribution functions of RF and truncation schemes are distinctly different from PME, the main difference being in the long-distance tail.

On the basis of these findings for lateral diffusion, velocity correlations, and lateral displacements in sections 3.3−3.5, we may conclude that the dynamics of lipid molecules in the plane of the membrane depend clearly on the treatment of electrostatic interactions. The RF and truncation schemes, in general, lead to results biased from those obtained by PME. These differences are apparent not only at large times, but they are pronounced even at short times (of the order of 1−10 ps) where l_{ave} is less than 10% of the size of the molecule. This allows us to settle the question posed in section 3.4 and conclude that the differences between different electrostatic schemes increase uniformly in time. Thus, *electrostatics plays a role at all time scales*, including even the very short ones where lateral diffusion corresponds to motion known as "rattling in a cage".

3.6. Rotational Diffusion. Besides lateral diffusion, the motion of lipid molecules can be described by their rotational degrees of freedom and characterized by the so-called rotational

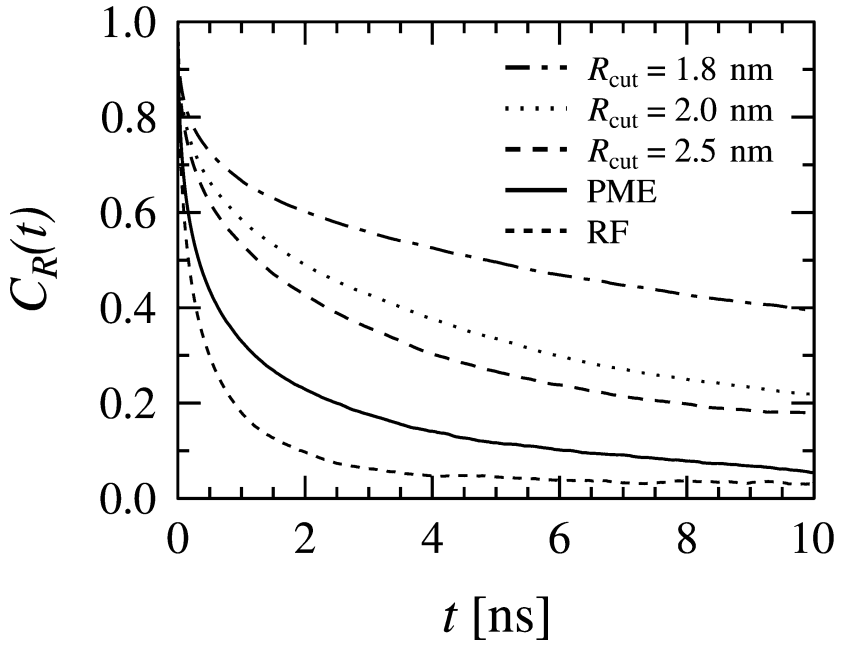

Figure 8. The correlation function of rotational diffusion $C_R(t)$ for the unit vector $\vec{\mu}(t)$ along the P−N vector in the headgroup of DPPC. At long times one expects $C_R(t) \sim \exp(-t/\tau_R)$.

diffusion coefficient D_R. To this end, one often considers Wigner rotation matrixes[69] such as the $C_2(t)$ correlation function

$$C_2(t) \equiv \frac{1}{2}\langle 3[\vec{\mu}(t)\vec{\mu}(0)]^2 - 1\rangle \qquad (7)$$

where $\vec{\mu}(t)$ is the unit vector of some chosen rotational mode at time t. At long times, one expects the decay $C_2(t) \sim \exp(-t/\tau_R)$ to yield the rotational diffusion coefficient via $\tau_R \propto 1/D_R$. This approach is particularly common in experiments such as the NMR technique.

In the present work, we have focused on three vectors that describe different aspects of rotational motion. First, we consider the P−N vector in the phosphocholine headgroup. Second, we examine the rotational diffusion of the glycerol group, characterized by a unit vector from the $sn-1$ carbon to the $sn-3$ carbon in a DPPC molecule (see Figure 1 in ref 36). Finally, we characterize the rotational diffusion of acyl chains, in which case the unit vector is drawn from the first to the last carbon in the $sn-1$ chain.

Results in Figure 8 demonstrate the decay of $C_2(t)$ for the P−N vector. At early times, the results from RF decay fastest of all, the half-time $t_{1/2}$ (defined as $C_2(t_{1/2}) = {}^1/_2$) being about 0.17 ns. The PME decays almost as rapidly, while the results based on truncation methods, on the other hand, decay much more slowly as is demonstrated by the value of $t_{1/2} = 4.9$ ns with $r_{cut} = 1.8$ nm. At longer times from 5 to 10 ns, we find $1/\tau_R = 0.143$ ns^{-1} for PME and 0.045 ns^{-1} for 1.8 nm.

Results for the characteristic times are summarized in Table 4. Largest deviations between PME and the truncation methods are found in the rotational time scales of the $sn-1$ tail. Then, both the early and the long time behavior deviate by a factor which ranges around *1 order of magnitude*.

The time scale of 50 ns studied in this work is not long enough to find the true asymptotic regime of $C_2(t)$. Much longer time scales would be needed to find the exponential regime for $C_2(t)$ with full certainty. Thus, the values in Table 4 should be regarded as suggestive. They do, however, allow us to compare the different schemes for the electrostatics, and the message is clear: *The dynamics of rotational motion in lipid bilayers is considerably influenced by the choice of electrostatic interactions*.

TABLE 4: Characteristic Times τ_R and $t_{1/2}$ (in Units of Nanoseconds) Describing the Decay of the Rotational Autocorrelation Function $C_R(t)$[a]

time	1.8 nm	2.0 nm	2.5 nm	PME	RF
			P−N Vector		
τ_R	22.2 ± 5.4	11.9 ± 2.2	12.1 ± 2.2	7.0 ± 0.5	2.1 ± 0.3
$t_{1/2}$	4.86 ± 0.70	1.88 ± 0.28	1.25 ± 0.12	0.33 ± 0.01	0.17 ± 0.01
			$sn-1$ Chain		
τ_R	243.0 ± 80.3	96.4 ± 18.9	89.4 ± 8.1	42.9 ± 6.6	41.0 ± 6.0
$t_{1/2}$	> 100	7.66 ± 3.10	2.32 ± 0.36	0.75 ± 0.01	0.36 ± 0.01
			Vector from $sn-1$ to $sn-3$		
τ_R	24.9 ± 5.9	16.5 ± 2.8	14.1 ± 2.0	10.2 ± 1.0	4.7 ± 0.6
$t_{1/2}$	3.77 ± 1.08	2.14 ± 0.70	1.49 ± 0.30	0.75 ± 0.04	0.28 ± 0.02

[a] Shown here are the times for the three vectors considered: the P−N vector, the vector from the first to the last carbon in the $sn-1$ chain, and the vector from the $sn-1$ carbon to the $sn-3$ carbon in the glycerol group. The times τ_R have been determined from the range between 5 and 10 ns.

3.7. Efficiency. As a final issue, let us briefly comment on the efficiency of RF and truncation schemes compared to PME. In the present model system without parallelization, we have found that the simulations with the RF method (using $r_{RF} = 0.9$ nm) are faster than with PME by a factor of 2.8. This advantage is important particularly in large systems, where the computational load becomes a major issue.

In the case of the truncation methods, a truncation of electrostatic interactions at 1.8 and 2.0 nm is faster than PME by a factor of 1.8 and 1.4, respectively. Truncation at 2.5 nm, however, is slightly slower than PME. This demonstrates that large truncation distances are not desirable in systems of present size, where the efficiency of PME is actually rather reasonable.

In general, the situation is more complicated. The CPU time needed for truncation schemes scales is $\mathcal{O}(N)$ or $\mathcal{O}(r_{cut}^3)$, while for PME it is $\mathcal{O}(N \log N)$. In addition to this, PME cannot be parallelized as efficiently as truncation methods. This implies that the truncation always becomes more efficient than PME as the size of the system or the number of parallel nodes is

increased. This idea applies to the RF method as well, since based on the present study the RF technique is almost as efficient as the truncation method. For $r_{RF} = r_{cut}$, the computational cost of using RF is about 10% larger than that of the truncation method. Thus, it is likely that the use of RF and truncation schemes will be inevitable in studies of large and complex systems, which are not doable by incorporating full electrostatics into the system in question.

4. Discussion and Summary

Together with current computational resources, the classical MD technique has very recently evolved to a stage where it can be applied to various dynamic processes in complex soft-matter systems. Fusion of liposomes with flat lipid bilayers and undulations of membranes are just two of the many examples in this regard. However, due to the large systems and long time scales involved in these processes, the computational effort of studying the dynamics is substantial. To reduce the computational cost, it has become common to handle the long-range component of electrostatic interactions through a RF correction, or to simply truncate the long-range electrostatic interactions. The latter choice, in particular, has been done despite the evidence that the truncation may affect structural properties of soft-matter systems and lead to substantial artifacts through unphysical pair correlations that change the phase behavior of the system.[36]

In this work, we have investigated the dynamics of DPPC lipid bilayers through multi-nanosecond MD simulations and compared the PME results with those of the RF technique and three different truncation schemes.

First of all, as for the truncation methods, we have found that the PME approach is clearly more costly as compared to the truncation schemes. For example, in the present model system, the computational cost of PME has been found to be larger by a factor of 1.8 compared to a truncation at 1.8 nm. At the same time, however, we have found strong evidence that the truncation of electrostatic interactions has a major disadvantage. The lateral diffusion rates studied using a truncation at 1.8 nm were found to deviate by 1 order of magnitude from the PME results. Similar deviations were found for all time scales studied, down to very short times where the lateral diffusion corresponds to short-scale motion known as "rattling in a cage". These problems certainly play a role in processes where lateral reorganization of molecules in a bilayer is important. The decay rate of the area per lipid fluctuations is changed almost as extensively, a feature which certainly affects the permeation rates of small molecules through membranes. As the other dynamic quantities considered in this work support these findings, we may conclude that the truncation is not the method of choice for incorporating electrostatic interactions into model systems of lipid membranes.

As for the RF technique, we have found that RF is a reasonable choice for electrostatics, though it suffers from certain features that are not easy to resolve. The problems are associated with the RF correction that does not account for changes in the environment around the charges studied. In particular, as the long-range correction is based on the use of a dielectric constant that is usually chosen to describe the bulk solvent, RF is not well suited for studies of interfaces such as membrane−water systems. In the present study, this is manifested in RDFs that differ in many details from the PME results (see section 3.1) and include a weak oscillating long-range tail not given by PME. While this effect can be reduced by increasing r_{RF}, this might not be sufficient. Perhaps the most important point, however, is the phase behavior given by the RF method. While we have found that the RDFs from RF are different from those obtained by PME, we have not observed actual artificial peaks in the RDFs due to the cutoff in the RF method. Also, the RDFs of the center of mass positions of the lipids given by RF and PME are by and large similar, and thus the phase behavior given by the RF technique seems to correspond to the fluid (liquid-crystalline) phase, as expected. Finally, while we have found that the RF results for dynamic quantities are considerably different from those obtained by PME, it is likely that this problem is due to the increased area per lipid $\langle A \rangle$ and could therefore be overcome by tuning some other details of the force field.

In all, considering the limitations of the RF method, we conclude that it is a reasonable and efficient description for electrostatics. While it is not as widely applicable for general applications as PME, the RF method offers a more solid and safer choice than the methods based on an abrupt truncation of electrostatics. However, there is no doubt that the PME approach is the method of choice of the methods considered in the present work, if the computational load is not a limiting factor.

We have found compelling evidence that the choice of a scheme for electrostatic interactions may dramatically affect the dynamical properties of lipids in a DPPC bilayer. While the present work serves as an example of various lipid membrane systems studied widely through similar MD techniques, one has to keep in mind that, strictly speaking, our results are specific to the present model. In general, the influence of the electrostatic scheme on the structure and dynamics depends on the force fields and other details chosen for the model in question. The influence of electrostatic schemes in other systems may therefore be different from the present one. Yet it is expected that our findings and conclusions apply to many other biologically relevant soft-matter systems, where electrostatics plays a crucial role; e.g., DNA−lipid complexes and proteins in membranes. The artificial ordering effects due to an abrupt truncation of electrostatic interactions exemplify this general problem, since the peaks and dips found when using this technique appear exactly at the truncation distance. Hence, if the electrostatics is not handled with care, one should be aware of possible artifacts in both the structure and the dynamics of the molecules studied.

Acknowledgment. This work has, in part, been supported by the Academy of Finland through its Center of Excellence Program (E.F. and I.V.), the National Graduate School in Materials Physics (E.F.), the Academy of Finland Grants Nos. 54113 (M.K.), 80851 (M.T.H.), and 80246 (I.V.), the Jenny and Antti Wihuri Foundation (M.T.H.), the Federation of Finnish Insurance Companies (M.T.H.), and by the European Union through the Marie Curie Fellowship HPMF-CT-2002-01794 (M.P.). We would also like to thank the Finnish IT Center for Science and the HorseShoe (DCSC) supercluster computing facility at the University of Southern Denmark for computer resources.

Supporting Information Available: Results for the particle displacement distribution function at several times from 10 ps to 10 ns and the RDFs for N−N, P−P, and CM−CM pairs for the RF and PME methods.

References and Notes

(1) Ladanyi, B. M.; Skaf, M. S. *Annu. Rev. Phys. Chem.* **1993**, *44*, 335−368.

(2) Koltover, I.; Salditt, T.; Rädler, J. O.; Safinya, C. R. *Science* **1998**, *281*, 78−81.

(3) Bandyopadhyay, S.; Tarek, M.; Klein, M. L. *J. Phys. Chem. B* **1999**, *103*, 10075−10080.
(4) Giudice, E.; Lavery, R. *Acc. Chem. Res.* **2002**, *35*, 350−357.
(5) Makarov, V.; Pettitt, B. M. *Acc. Chem. Res.* **2002**, *35*, 376−384.
(6) Grosberg, A. Y.; Nguyen, T. T.; Shklovskii, B. I. *Rev. Mod. Phys.* **2002**, *74*, 329−345.
(7) Patra, M.; Patriarca, M.; Karttunen, M. *Phys. Rev. E* **2003**, *67*, 031402.
(8) Bloom, M.; Evans, E.; Mouritsen, O. G. *Q. Rev. Biophys.* **1991**, *24*, 293−397.
(9) *Structure and Dynamics of Membranes: From Cells to Vesicles*; Lipowsky, R., Sackmann, E., Eds.; Elsevier: Amsterdam, 1995.
(10) *Biological Membranes: A Molecular Perspective from Computation and Experiment*; Merz, K. M., Jr., Roux, B., Eds.; Birkhäuser: Boston, 1996.
(11) Nagle, J. F.; Tristram-Nagle, S. *Biochim. Biophys. Acta* **2000**, *1469*, 159−195.
(12) *Lipid Bilayers: Structure and Interactions*; Katsaras, J., Gutberlet, T., Eds.; Springer-Verlag: Berlin, 2001.
(13) Langer, R. *Nature* **1998**, *392*, 5−10.
(14) Needham, D. *MRS Bull.* **1999**, *24*, 32−40.
(15) Frenkel, D.; Smit, B. *Understanding Molecular Simulation: From Algorithms to Applications*, 2nd ed.; Academic Press: San Diego, 2002.
(16) Saiz, L.; Bandyopadhyay, S.; Klein, M. L. *Biosci. Rep.* **2002**, *22*, 151−173.
(17) Tobias, D. J. *Curr. Opin. Struct. Biol.* **2001**, *11*, 253−261.
(18) Sagui, C.; Darden, T. A. *Annu. Rev. Biophys. Biomol. Struct.* **1999**, *28*, 155−179.
(19) Greengard, L.; Rokhlin, V. *J. Comput. Phys.* **1987**, *73*, 325−348.
(20) Essman, U.; Perera, L.; Berkowitz, M. L.; Darden, H. L. T.; Pedersen, L. G. *J. Chem. Phys.* **1995**, *103*, 8577−8592.
(21) Allen, M. P.; Tildesley, D. J. *Computer Simulation of Liquids*; Clarendon Press: Oxford, 1987.
(22) Zangi, R.; de Vocht, M. L.; Robillard, G. T.; Mark, A. E. *Biophys. J.* **2002**, *83*, 112−124.
(23) Marrink, S. J.; Lindahl, E.; Edholm, O.; Mark, A. E. *J. Am. Chem. Soc.* **2001**, *123*, 8638−8639.
(24) Marrink, S. J.; Tieleman, D. P. *Biophys. J.* **2002**, *83*, 2386−2392.
(25) Alper, H. E.; Levy, R. M. *J. Chem. Phys.* **91**, 1242−1251.
(26) Feller, S. E.; Pastor, R. W.; Rojnuckarin, A.; Bogusz, A.; Brooks, B. R. *J. Phys. Chem.* **100**, 17011−17020.
(27) Mark, P.; Nilsson, L. *J. Comput. Chem.* **2002**, *23*, 1211−1219.
(28) Alper, H. E.; Bassolino, D.; Stouch, T. R. *J. Chem. Phys.* **98**, 9798−9807.
(29) Alper, H. E.; Bassolino-Klimas, D.; Stouch, T. R. *J. Chem. Phys.* **99**, 5547−5559.
(30) Smith, P. E.; Pettitt, B. M. *J. Chem. Phys.* **1991**, *95*, 8430−8441.
(31) Schreiber, H.; Steinhauser, O. *Biochemistry* **1992**, *31*, 5856−5860.
(32) York, D. M.; Darden, T. A.; Pedersen, L. G. *J. Chem. Phys.* **99**, 8345−8348.
(33) York, D. M.; Yang, W.; Lee, H.; Darden, T.; Pedersen, L. G. *J. Am. Chem. Soc.* **1995**, *117*, 5001−5002.
(34) Norberg, J.; Nilsson, L. *Biophys. J.* **2000**, *79*, 1537−1553.
(35) Venable, R. M.; Brooks, B. R.; Pastor, R. W. *J. Chem. Phys.* **2000**, *112*, 4822−4832.
(36) Patra, M.; Karttunen, M.; Hyvönen, M.; Falck, E.; Lindqvist, P.; Vattulainen, I. *Biophys. J.* **2003**, *84*, 3636−3645.
(37) Tieleman, D. P.; Marrink, S. J.; Berendsen, H. J. C. *Biochim. Biophys. Acta* **1997**, *1331*, 235−270.
(38) Anézo, C.; de Vries, A. H.; Höltje, H.-D.; Tieleman, D. P.; Marrink, S. J. *J. Phys. Chem. B* **2003**, *107*, 9424−9433.
(39) Tieleman, D. P.; Berendsen, H. J. C. *J. Chem. Phys.* **1996**, *105*, 4871−4880.
(40) Berger, O.; Edholm, O.; Jahnig, F. *Biophys. J.* **1997**, *72*, 2002−2013.
(41) Berendsen, H. J. C.; Postma, J. P. M.; van Gunsteren, W. F.; Hermans, J. In *Intermolecular Forces*; Pullman, B., Ed.; Reidel: Dordrecht, 1981; pp 331−342.
(42) Bishop, T. C.; Skeel, R. D.; Schulten, K. *J. Comput. Chem.* **1997**, *18*, 1785−1791.
(43) Sum, A. K.; Faller, R.; de Pablo, J. J. *Biophys. J.* **2003**, *85*, 2830−2844.
(44) Sum, A. K.; de Pablo, J. J. *Biophys. J.* **2003**, *85*, 3636−3645.
(45) Tieleman, D. P.; Hess, B.; Sansom, M. S. P. *Biophys. J.* **2002**, *83*, 2393−2407.
(46) Lindahl, E.; Hess, B.; van der Spoel, D. 2001. *J. Mol. Model.* **2001**, *7*, 306−317.
(47) Berendsen, H. J. C.; Postma, J. P. M.; van Gunsteren, W. F.; DiNola, A.; Haak, J. R. *J. Chem. Phys.* **1984**, *81*, 3684−3690.
(48) Hess, B.; Bekker, H.; Berendsen, H. J. C.; Fraaije, J. G. E. M. *J. Comput. Chem.* **1997**, *18*, 1463−1472.
(49) Mashl, R. J.; Scott, H. L.; Subramaniam, S.; Jakobsson, E. *Biophys. J.* **2001**, *81*, 3005−3015.
(50) Smondyrev, A. M.; Berkowitz, M. L. *Biophys. J.* **2001**, *80*, 1649−1658.
(51) Moore, P. B.; Lopez, C. F.; Klein, M. L. *Biophys. J.* **2001**, *81*, 2484−2494.
(52) Feller, S. E.; Gawrisch, K.; MacKerell, A. D., Jr. *J. Am. Chem. Soc.* **2001**, *124*, 318−326.
(53) Lindahl, E.; Edholm, O. *Biophys. J.* **2000**, *79*, 426−433.
(54) Marrink, S. J.; Mark, A. E. *J. Phys. Chem. B* **2001**, *105*, 6122−6127.
(55) Shinoda, W.; Okazaki, S. *J. Chem. Phys.* **109**, *109*, 1517−1521.
(56) Almeida, P. F. F.; Vaz, W. L. C. In *Structure and Dynamics of Membranes: From Cells to Vesicles*; Lipowsky, R., Sackmann, E., Eds.; Elsevier: Amsterdam, 1995; pp 305−357.
(57) Vattulainen, I.; Mouritsen, O. G. In *Diffusion in Condensed Matter*; Kärger, J., Heitjans, P., Haberland, R., Eds.; Springer-Verlag: Berlin, 2003, In Press.
(58) Hansen, J.-P.; McDonald, I. R. *Theory of Simple Liquids*, 2nd ed.; Academic Press: San Diego, 2000.
(59) Cohen, M. H.; Turnbull, D. *J. Chem. Phys.* **1959**, *31*, 1164−1169.
(60) Macedo, P. B.; Litovitz, T. A. *J. Chem. Phys.* **1964**, *42*, 245−256.
(61) Filippov, A.; Orädd, G.; Lindblom, G. *Biophys. J.* **2003**, *84*, 3079−3086.
(62) Hyvönen, M. T.; Kovanen, P. T. *J. Phys. Chem. B* **2003**, *107*, 9102−9108.
(63) Almeida, P. F. F.; Vaz, W. L. C.; Thompson, T. E. *Biochemistry* **1992**, *31*, 6739−6747.
(64) Korlach, J.; Schwille, P.; Webb, W. W.; Feigenson, G. W. *Proc. Natl. Acad. Sci. U. S. A.* **1999**, *96*, 8461−8466.
(65) Vaz, W. L. C.; Clegg, R. M.; Hallmann, D. *Biochemistry* **1985**, *24*, 781−786.
(66) König, S.; Pfeiffer, W.; Bayerl, T.; Richter, D.; Sackmann, E. *J. Phys. II France* **1992**, *2*, 1589−1615.
(67) Sackmann, E. In *Structure and Dynamics of Membranes: From Cells to Vesicles*; Lipowsky, R., Sackmann, E., Eds.; Elsevier: Amsterdam, 1995; pp 213−304.
(68) Tabony, J.; Perly, B. *Biochim. Biophys. Acta* **1990**, *1063*, 67−72.
(69) Pastor, R. W.; Feller, S. E. In *Biological Membranes: A Molecular Perspective from Computation and Experiment*; Merz, K. M., Jr., Roux, B., Eds.; Birkhäuser: Boston, 1996; pp 3−29.